First-principles calculations of the structural stability and magnetic property of the metastable phases in the equilibrium immiscible Co–Au system

2006 J. Phys.: Condens. Matter 18 4345

(http://iopscience.iop.org/0953-8984/18/17/020)

INSTITUTE OF PHYSICS PUBLISHING JOURNAL OF PHYSICS: CONDENSED MATTER

J. Phys.: Condens. Matter **18** (2006) 4345–4353 doi:10.1088/0953-8984/18/17/020

First-principles calculations of the structural stability and magnetic property of the metastable phases in the equilibrium immiscible Co–Au system

Y Kong, L T Kong and B X Liu[1]

Advanced Materials Laboratory, Department of Materials Science and Engineering, Tsinghua University, Beijing 100084, People's Republic of China
and
State Key Laboratory of Solid-State Microstructure, Nanjing University, Nanjing 200039, People's Republic of China

E-mail: dmslbx@tsinghua.edu.cn

Received 30 November 2005, in final form 27 March 2006
Published 13 April 2006
Online at stacks.iop.org/JPhysCM/18/4345

Abstract

To reveal the energetic sequence of the alloy phases in the Co–Au system, the lattice constants, cohesive energies, and bulk modulus of the fcc Au, hcp Co, the B1, B2, and $L1_0$ structured CoAu phases, and the $D0_3$, $L1_2$, and $D0_{19}$ structured Co_3Au and $CoAu_3$ phases, respectively, are acquired by first-principles calculations within the generalized-gradient approximation (GGA) as well as within the local density approximation (LDA). In addition, the magnetic moment of the Co atom in the studied phases are also calculated. To further examine the structural stability, the elastic constants of the studied phases are calculated and the results suggest that the fcc-type structures could be elastically stable at Co/Au = 1:3, 1:1, and 3:1, whereas the hcp-type structures could be stable at Co/Au = 1:3 and 3:1. Moreover, the spatial valence charge density (SVCD) and spin density of the studied phases are also calculated to clarify the physical origin of the structural stability. It turns out that, in the relatively stable phases, the high SVCDs mostly distribute between the similar atoms, thus forming the attractive covalent bonding to stabilize the respective structures, and that the spin density may also play an important role in influencing the stability of the ferromagnetic metastable phases.

(Some figures in this article are in colour only in the electronic version)

1. Introduction

The magnetism of solid/condensed matter has long been one of the most important scientific issues from both fundamental and practical points of view. Recently, some new magnetic

[1] Author to whom any correspondence should be addressed.

phases which are not present in nature have been obtained by some nonequilibrium materials processing techniques [1–5]. For instance, Velu *et al* have successfully grown Co/Au(111) multilayers, which exhibited unique perpendicular magnetic anisotropy [1]. Izquierdo *et al* have grown the bcc cobalt epitaxially on a GaAs(110) substrate by using Sb as a surfactant and found an improvement on the magnetic response in the obtained bcc Co thin films [2]. Besides, some Co-based bulk glassy alloys have been produced and the alloys featured an ultrahigh strength behaviour and soft magnetic properties [3]. In theoretical studies, Hafner *et al* [6–10] systematically studied the structure, electronic, and magnetic properties of metallic glasses containing the ferromagnetic Fe, Co, Ni elements.

The foregoing experimental and/or theoretical studies have concentrated mostly on the ferromagnetic elements or their equilibrium alloys, whereas equilibrium immiscible systems containing ferromagnetic elements have been studied less and have attracted much research interest in recent years. In this respect, a few of the preliminary works of the immiscible systems containing ferromagnetic elements have shown some interesting results. For example, very recently, Ferrando *et al* [11] figured out that, with substantial intermixing of both components, chemical bonding of the strong directionality of the Au–Au moved the maximum in the stability of the bimetallic Au–Co clusters. Moreover, their calculation results further confirmed the strong tendency for mixing of the small bimetallic clusters, even for those that presented a very strong tendency against mixing in the bulk phase (such as Ag–Ni, Ag–Co, or Au–Co with positive heat of formation). Kong *et al* [12] studied the magnetic properties of the nonequilibrium structures in the immiscible Co–Ag system, and found that the variation of the magnetic moment of Co was governed by a combining effect of two competitive factors, i.e., atomic volume expansion enhanced the magnetic moment of the Co atom, whereas Ag alloying reduced the magnetic moment of the Co atom.

The metastability, i.e. the structural stability of the artificially created nonequilibrium phases (or metastable phases), is of vital importance from both theoretical and practical points of view. In the present study, we perform first-principles calculations to study some hypothetical crystalline structures in an equilibrium immiscible model system, i.e., the Co–Au system with a positive heat of formation $\Delta H = +10$ kJ mol^{-1} [13], through exploring the short-range bonding of local chemical or topological packing structures. The objective of the present study is to reveal the underlying physics of the metastability, and to determine the magnetic moment of the Co atom in the metastable phases.

2. First-principles calculation methods

The well-established *ab initio* simulation software called CASTEP [14] is employed in the present first-principles calculations. For each phase of interest, the geometry optimization is first performed to find its ground state, as well as to obtain the lattice constants, cohesive energies, bulk moduli and magnetic moments. Second, the elastic constants are calculated on the basis of the results of the geometry optimization. The calculations are conducted in a plane-wave basis, with a maximum plane-wave cut-off energy of 330 eV. The pseudo-atomic configurations adopted for Co and Au are 3d7 4s2 and 5d10 6s1, respectively. The exchange and correlation energy is described by the generalized-gradient approximation (GGA) using the Perdew–Wang 1991 (PW91) potentials [15] and the local density approximation (LDA) using the Ceperley and Alder data, as parameterized by Perdew and Zunger [16], respectively. Integration in the Brillouin zone (BZ) is performed on the special k points determined from the Monkhorst–Pack scheme [17]. Geometry optimization is conducted using the Broyden–Fletcher–Goldfarb–Shanno (BFGS) method [18].

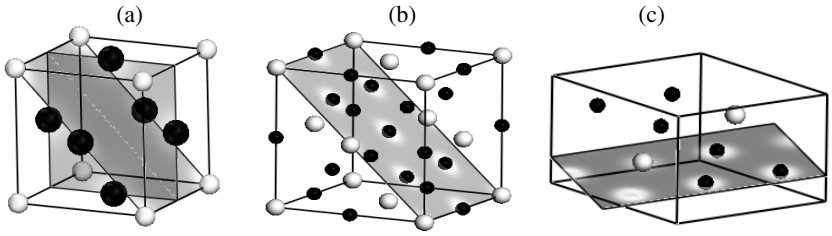

Figure 1. The crystalline structure of (a) $L1_2$, (b) $D0_3$, and (c) $D0_{19}$, respectively. The black balls represent the major alloy element, while the gray balls represent the minor alloy element. The slice shown in (c) is used for visualization in figure 4.

Since it is known that the GGA may promote magnetism, for all the studied hypothetical phases of the immiscible Co–Au systems, both the GGA and LDA spin-polarized calculations are performed for comparison. The spin-polarized self-consistent calculations are started at an assigned magnetic moment $\mu_{Co} = 2\ \mu_B$ per Co atom, so that the iteration should lead to a low-spin solution, if it exists. The obtained results of the spin-polarized calculations are different for the three studied chemical stoichiometries. At the chemical stoichiometry of Co/Au = 1:3, the magnetic moments are quite large, while at the chemical stoichiometries of Co/Au = 1:1 and 1:3, the magnetic effect can be ignored, as the initially assigned magnetic moments eventually become a value quite close to zero.

3. Results and discussion

3.1. Structural parameters

The bcc-type $D0_3$ (i.e. BiF_3 type), fcc-type $L1_2$ (i.e. Cu_3Au type), and hcp-type $D0_{19}$ (i.e. Ni_3Sb type) structures are chosen as the hypothetical crystalline structures for the possible nonequilibrium $CoAu_3$ and Co_3Au phases. The corresponding $D0_3$, $L1_2$, and $D0_{19}$ crystalline structures are shown in figure 1. The cubic B1 (i.e. NaCl type), bcc-type B2 (i.e. CsCl type), and tetragonal-type $L1_0$ (i.e. CuAu type, which can be regarded as a distorted fcc structure with $a = b \neq c$) structures are selected as the hypothetical crystalline structures for the possible nonequilibrium CoAu phases.

The calculated lattice constants (a and c), average atomic volume (vol/atom), the minimum total energy (ΔE) of the hypothetical crystalline structures by taking $L1_2$ as a reference state, and the bulk modulus (B) of the fcc Au, hcp Co and the nine hypothetical crystalline structures of the equilibrium immiscible Co–Au system are listed in table 1.

From table 1, one sees that, either within GGA or LDA, at a chemical stoichiometry of Co/Au = 1:3 (or 3:1), the $D0_{19}$ structure has the lowest energy, while the energies of $L1_2$ and $D0_{19}$ structures are quite close to each other, and the energy of the $D0_3$ structure is a little higher than $L1_2$ and $D0_{19}$. At the chemical stoichiometry of Co/Au = 1:1, the $L1_0$ structure has the lowest energy. From table 1, one also sees that, by increasing the Au concentration, the average atom volume is expanded. This trend is reasonable, as the average atomic volume of hcp Co is 11.16 $Å^3$/atom, while that of fcc Au is 18.05 $Å^3$/atom. For the bulk modulus, one sees that, in contrast to the average atomic volume, the bulk modulus decreases with increasing Au concentration. The calculated results show that the lattice constants obtained within LDA are always smaller than those obtained within GGA in a specific phase, while the bulk moduli show the opposite trend.

Table 1. The calculated lattice constants a and c, average atomic volume V, total energy difference ΔE_c, bulk modulus B, and magnetic moments (MM) of the fcc Au, hcp Co, and the nine hypothetical crystalline structures of the Co–Au system. The data in the upper row are obtained within GGA and the data in the lower row are obtained within LDA. While, for Au and Co, the data in the third row are some experimental data taken from [22].

		a (Å)	c (Å)	Vol (Å^3/atom)	ΔE_c (eV/atom)	B (GPa)	MM (μ_B)
Au	fcc	4.164		18.05		147.85	
		4.082		17.00		197.24	
		4.08				173.2	
$CoAu_3$	$D0_3$	6.418		16.53	0.027	154.78	
		6.286		15.52	0.076	203.19	
	$L1_2$	4.035		16.42	0.000	158.72	
		3.952		15.43	0.000	205.64	
	$D0_{19}$	2.849	4.675	16.43	−0.041	155.90	
		2.788	4.584	15.43	−0.026	206.50	
CoAu	B1	5.106		16.64	0.893	135.12	
		4.987		15.50	1.084	172.70	
	B2	3.070		14.48	0.022	177.42	
		3.005		13.57	0.019	232.27	
	$L1_0$	4.022	3.585	14.50	0.000	177.97	
		3.915	3.546	13.59	0.000	233.01	
Co_3Au	$D0_3$	5.965		13.26	0.473	176.43	1.7951
		5.783		12.08	1.262	261.70	0.2503
	$L1_2$	3.731		12.99	0.000	190.85	1.7423
		3.647		12.13	0.000	248.90	1.7258
	$D0_{19}$	2.654	4.253	12.97	−0.149	166.49	1.7265
		2.597	4.139	12.08	−0.189	241.15	1.6814
Co	hcp	2.513	4.081	11.16		225.45	1.6022
		2.453	3.962	10.33		268.05	1.5202
		2.51	4.07			191.4	1.72

3.2. Magnetic moment and partial spin-polarized electronic density of states

The obtained magnetic moments within both the GGA and LDA, for the hcp Co and the $D0_3$, $L1_2$, and $D0_{19}$ structured Co_3Au phases, are also listed in table 1 and shown in figure 2. From the calculated results, one finds that, within the GGA (the square symbols in figure 2) the increasing sequence of magnetic moment per Co atom is hcp Co, $D0_{19}$ Co_3Au, $L1_2$ Co_3Au, and $D0_3$ Co_3Au. Such a trend of increasing magnetic moment corresponds with the expansion of the average atomic volume. While within the LDA (the round symbols in figure 2), the calculated magnetic moment per Co atom are all lower than those in GGA, and even falls to 0.2503 μ_B in the $D0_3Co_3Au$ phase, which is very small compared to that obtained from the GGA.

To find out the underlying physics of the magnetic moment of Co in Co_3Au phases, the partial spin-polarized electronic density of states (DOS) of Co in these three crystalline structures is computed and then compared with the spin-polarized DOS of the pure hcp Co, respectively. The obtained results are shown in figure 3, where the dotted line is the spin-polarized DOS of pure hcp Co and the solid and dashed lines are the DOS of Co in $D0_{19}$, $L1_2$, and $D0_3$ structures calculated within GGA and LDA, respectively, from (a) to (c). From figure 3, one can see that, while within the GGA (the solid lines), with increasing average

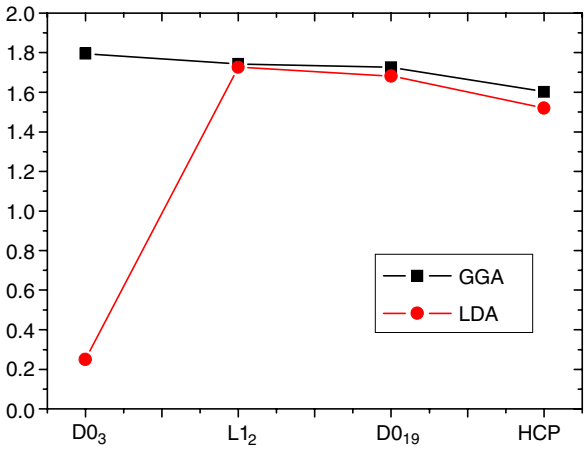

Figure 2. The magnetic moments obtained from first-principles calculations within GGA as well as LDA, for the hcp Co and the $D0_3$, $L1_2$, and $D0_{19}$ structured Co_3Au phases, respectively.

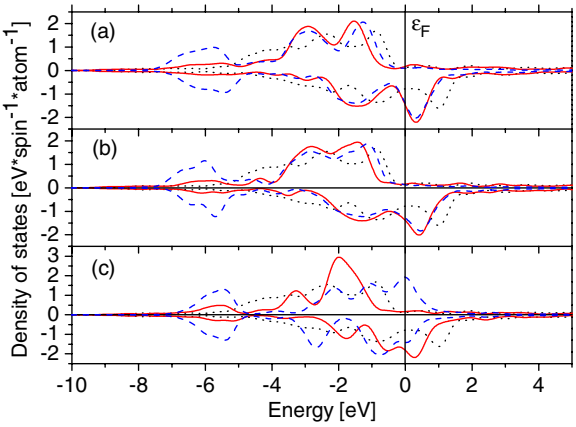

Figure 3. The calculated density of states of Co atoms in (a) $D0_{19}$, (b) $L1_2$, and (c) $D0_3$ structured Co_3Au phases, respectively, compared to that of Co atoms in the equilibrium hcp Co. Where the solid lines represent the results of GGA, the dashed lines represent the results of LDA, and the dotted lines represent the results of GGA of hcp Co.

atomic volume, the spin-polarized DOS is narrowed and increased around the Fermi level. Within the LDA (the dashed lines), for $L1_2$ and $D0_{19}$ structures, there appear many up and down spin-polarized electrons around -6 eV in energy, so that the DOS of spin-polarized electrons around the Fermi level decreases. For $D0_3$ Co_3Au within the LDA, the up and down spin-polarized electrons are almost equally accumulated at the Fermi level, resulting in a sharp decrease in the total magnetic moment compared to that within the GGA.

It is known that for the Co element, because of its open d shells, isolated transition metal Co ions possess large magnetic moments governed by Hund's rules. While in bulk transition metal phases, the crystal field quenches the free ion orbital momentum, thus reducing the magnetic moment of the Co element [4]. Consequently, in bulk phases, a larger atomic volume leads to smaller interactions among the atoms. In such an environment, the Co ions could behave more like isolated ions, thus leading to the enhanced magnetic moments.

Table 2. The elastic constants (GPa) of nine hypothetical crystalline structures in the Co–Au system calculated from CASTEP. The data in the upper row are obtained within GGA and the data in the lower row are obtained within LDA.

		C_{11}	C_{12}	C_{44}	C_{13}	C_{33}	C'
$CoAu_3$	$D0_3$	144.25	160.05	86.98			−7.90
		189.60	209.99	114.20			−10.19
	$L1_2$	174.27	150.94	41.45			11.66
		236.94	189.99	68.65			23.47
	$D0_{19}$	199.70	146.62	24.97	119.08	234.45	26.54
		293.65	182.39	38.49	148.73	312.34	55.63
CoAu	B1	335.05	35.15	−9.56			149.95
		431.03	43.54	−7.33			193.74
	B2	168.43	181.92	114.26			−6.745
		223.22	236.78	148.99			−6.78
	$L1_0$	241.21	124.17	102.79	172.24	195.36	28.26
		307.99	170.01	128.04	220.20	260.41	14.02
Co_3Au	$D0_3$	126.22	201.54	66.75			−37.66
		186.47	299.32	91.00			−56.42
	$L1_2$	279.35	146.60	116.27			66.37
		361.39	192.65	151.76			84.37
	$D0_{19}$	216.73	153.75	74.82	113.71	315.16	31.49
		372.61	197.70	86.19	158.20	397.44	87.45

In short, according to the calculations within the GGA and LDA, the magnetic moment of Co atoms in $L1_2$ and $D0_{19}$ structured Co_3Au phases are enhanced compared to pure hcp Co, while for the $D0_3$ structured Co_3Au phase, the GGA and LDA give different results, that is, the magnetic moment of Co atoms in $D0_3$ structured Co_3Au is enhanced within GGA, yet is predicted to be small within LDA.

3.3. Elastic constants

To examine the elastic stability, the elastic constants of the nine hypothetical crystalline structures of the Co–Au system are also calculated using CASTEP. The results obtained are listed in table 2, in which both the GGA and LDA calculation results are included. It is noted that the elastic constants obtained from LDA are commonly higher than those obtained from GGA.

From table 2, one also sees some unusual features in the elastic constants. First, for the chemical stoichiometries of $CoAu_3$ and Co_3Au, the fcc-type $L1_2$ structured $CoAu_3$ and Co_3Au phases may be elastically metastable, as their elastic constants are all positive. Similarly, the hcp-type $D0_{19}$ structured $CoAu_3$ and Co_3Au may also be metastable. However, the shear elastic constant $C' = (C_{11} - C_{12})/2$ of the $D0_3$ structure is negative, implying that the $D0_3$ structured $CoAu_3$ phase is dynamically unstable under elastic shearing. Second, for chemical stoichiometry of Co/Au = 1:1, the $L1_0$ CoAu may be elastically stable, while the B1 and B2 structured CoAu are both unstable. In summary, the fcc-type structures are all stable for Co/Au = 1:3, 1:1, and 3:1, while the hcp-type structures are also stable for Co/Au = 1:3 and 3:1.

It is of interest to compare the predictions based on first-principles calculations with the experimental observations. In ion beam mixing experiments, Tsaur *et al* [19] have observed the single-phase metastable fcc solid solutions in the composition range of 100 at.% to 5 at.% Au (i.e. up to 95 at.% Co), and an amorphous alloy at $Au_{25}Co_{75}$, which transformed into a metastable fcc phase upon thermal annealing at ∼200 °C. Obviously, these observations could

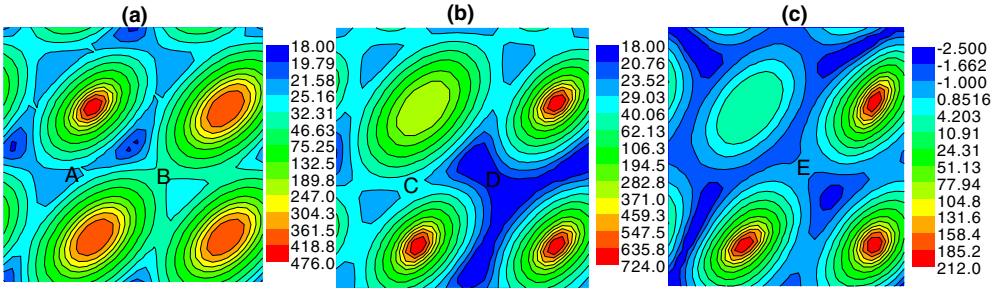

Figure 4. Visualization of the spatial valence charge density of (a) $D0_{19}$ $CoAu_3$ and (b) $D0_{19}$ Co_3Au, respectively, together with a visualization of the spin density of (c) $D0_{19}$ Co_3Au. In each structure, the slice is the (001) plane, in which there are three Co atoms and one Au atom. The unit is the number of electrons per cell. The letters indicate the interaction areas.

provide some support for the relevance of the above predictions based on the first-principles calculations.

The above calculated results raise some interesting issues, i.e. why the Co–Au system shows such dynamical behaviour, and what is the effect of the magnetism on the structural stability of the metastable phases?

3.4. Physical origin of the structural stability

To achieve an answer, we calculate the spatial valence charge density (SVCD) and the spin density, to reveal the bonding and magnetic nature in the phases studied. We use slices of some specific planes (shown in figure 1 for corresponding crystalline structures) in the electronic density field to show the details of the SVCD and the spin density in a quantitative way. The slice is plotted with colour filled contours between the minimum and maximum charge density and spin density. The maxima in the electronic density field correspond to the positions of the atoms that have semi-core states, which are treated explicitly as valence.

As a typical example, we only show the contour plots of the details of the SVCD of the $D0_{19}$ structured $CoAu_3$ and Co_3Au within GGA, and the contour plots of the details of the spin density of the $D0_{19}$ structured Co_3Au in figure 4, in which the letters indicate the interaction areas. As clarified by the calculated elastic constants, the $D0_{19}$ structured $CoAu_3$ and Co_3Au phases can be metastable. For the metastable $D0_{19}CoAu_3$ (figure 4(a)), one can find that there is obviously much stronger electronic interaction between similar Au atoms (B area in the figure) than between dissimilar Co–Au atoms (A area), and such electron interaction between the similar Au atoms could be considered to be an additional covalent bonding, helping to stabilize the $D0_{19}$ $CoAu_3$ structure. For the $D0_{19}$ Co_3Au (figure 4(b)), one can see that, in contrast to the $D0_{19}$ $CoAu_3$ structure, there is almost no electronic interaction between similar Co atoms (D area), while the electronic interaction between dissimilar Co–Au atoms (C area) is prominent. As it is ferromagnetic, however, besides the electrostatic interaction, the spin-polarized interaction should also be considered. We therefore calculated the spin density of spin-polarized $D0_{19}$ Co_3Au using CASTEP and the detailed contour plot is shown in figure 4(c). From figure 4(c), one can see that, when considering spin polarization, there is spin-polarized interaction between similar Co atoms (E area), which offers an attractive force to help in stabilizing the $D0_{19}$ Co_3Au structure.

In short, in the relatively stable $D0_{19}$ structured $CoAu_3$ phase, there are large enough SVCDs located between the similar Au–Au atoms, which leads to strong attractive interactions.

Whereas in the $D0_{19}$ structured Co_3Au phase, the high SVCDs only distribute between the dissimilar Co–Au atoms. Nonetheless, when considering the spin polarization in the $D0_{19}$ structured Co_3Au, the spin-polarized interaction offers an additive attractive force to stabilize the $D0_{19}$ structure.

It follows that the attractive covalent bonding between similar atoms helps in stabilizing the structures, and that the spin density may also play an important role in influencing the structural stability of the ferromagnetic metastable phases. The above discussion may also explain why some kinds of amorphous structure or homogeneity of a supersaturated solid solution is obtained experimentally between the immiscible metallic elements, and that the atomic-level topology shown is phase separated [20, 21]. That is to say, since the electronic interaction between similar atoms can stabilize an alloy phase, when the similar atoms segregate to some extent there can appear some new phase in the equilibrium immiscible systems.

4. Conclusion remarks

First, the calculated cohesive energies within GGA and LDA using CASTEP both suggest that, at Co/Au = 3:1 and 1:3, the $D0_{19}$ structure has the lowest energy, while the energies of $L1_2$ and $D0_{19}$ structures are quite close, and that, at Co/Au = 1:1, the $L1_0$ structure has the lowest energy.

Second, the calculated elastic constants within GGA and LDA from CASTEP both suggest that the fcc-type structures are all elastically stable at Co/Au = 1:3, 1:1, and 3:1, and that the hcp-type structures are only stable at Co/Au = 1:3 and 3:1.

Third, it is found that the high SVCDs distribute mostly between similar atoms in the relatively stable phases, suggesting that the attractive covalent bonding between similar atoms helps in stabilizing the respective structures.

Fourth, it is also found that the spin density may also play an important role in influencing the structural stability of the ferromagnetic metastable phases.

Acknowledgment

The authors are grateful for financial support from the National Natural Science Foundation of China, The Ministry of Science and Technology of China (G20000672), and from Tsinghua University.

References

[1] Velu E, Dupas C, Renard D, Renard J P and Seiden J 1988 *Phys. Rev.* B **37** 668
[2] Izquierdo M, Davila M E, Avila J, Ascolani H, Teodorescu C M, Martin M G, Franco N and Chrost J 2005 *Phys. Rev. Lett.* **94** 187601
[3] Inoue A, Shen B, Koshiba H, Kato H and Yavari A R 2003 *Nat. Mater.* **2** 661
[4] Khmelevskyi S, Mohn P, Redinger J and Weinert M 2005 *Phys. Rev. Lett.* **94** 146403
[5] Prokhnenko O, Kamarad J, Prokes K, Arnold Z and Andreev A V 2005 *Phys. Rev. Lett.* **94** 107202
[6] Spisak D, Becker Ch and Hafner J 1995 *Phys. Rev.* B **51** 11616
[7] Becker Ch and Hafner J 1994 *Phys. Rev.* B **50** 3913
[8] Hafner J, Tegze M and Becker Ch 1994 *Phys. Rev.* B **49** 285
[9] Hausleitner Ch and Hafner J 1993 *Phys. Rev.* B **47** 5689
[10] Hausleitner Ch and Hafner J 1992 *Phys. Rev.* B **45** 128
[11] Ferrando R, Fortunelli A and Rossi G 2005 *Phys. Rev.* B **72** 085449
[12] Kong L T, Zhang R F, Li Z C and Liu B X 2003 *Phys. Rev.* B **68** 134446
[13] De Boer F R, Boom R, Mattens W C M, Miedema A R and Niessen A K 1989 *Cohesion in Metals: Transition Metal Alloys* (Amsterdam: North-Holland)

[14] Segall M D, Lindan P L D, Probert M J, Pickard C J, Hasnip P J, Clark S J and Payne M C 2002 *J. Phys.: Condens. Matter* **14** 2717
[15] Perdew J P and Wang Y 1992 *Phys. Rev.* B **45** 13244
[16] Perdew J P and Zunger A 1981 *Phys. Rev.* B **23** 5048
[17] Monkhorst H J and Pack J D 1976 *Phys. Rev.* B **13** 5188
[18] Fischer T H and Almlof J 1992 *J. Phys. Chem.* **96** 9768
[19] Tsaur B Y, Lau S S, Hung L S and Mayer J W 1981 *Nucl. Instrum. Methods* **182/183** 67
[20] He J H, Sheng H W, Lin J S, Schilling P J, Tittsworth R C and Ma E 2002 *Phys. Rev. Lett.* **89** 125507
[21] He J H, Sheng H W, Schilling P J, Chien C-L and Ma E 2001 *Phys. Rev. Lett.* **86** 2826
[22] Kittel C 1996 *Introduction to Solid State Physics* (New York: Wiley)